Zn2+ leakage and photo-induced reactive oxidative species do not explain the full toxicity of ZnO core Quantum Dots

Xavier Bellanger, Raphaël Schneider, Clément Dezanet, Boussad Arroua, Lavinia Balan, Patrick Billard, Christophe Merlin

Zn^{2+} leakage and photo-induced reactive oxidative species do not explain the full toxicity of ZnO core Quantum Dots

Xavier Bellanger [a], Raphaël Schneider [b*], Clément Dezanet [b], Boussad Arroua [a], Lavinia Balan [c], Patrick Billard [d], Christophe Merlin [a*]

[a] Université de Lorraine, CNRS, LCPME, F-54000 Nancy, France.

[b] Université de Lorraine, CNRS, LRGP, F-54000 Nancy, France.

[c] Institut de Science des Matériaux de Mulhouse (IS2M), CNRS, UMR 7361, 15 rue Jean Starcky, 68093 Mulhouse, France

[d] Université de Lorraine, CNRS, LIEC, F-54000 Nancy, France

* to whom correspondence should be addressed

KEYWORDS. Metal oxide nanoparticles; ZnO Quantum Dots; Nanotoxicity; Photo-induced Reactive oxygen species; Cell surface damages.

ABSTRACT

Metal oxide nanoparticles (NPs), and among them metal oxides Quantum Dots (QDs), exhibit a multifactorial toxicity combining metal leaching, oxidative stress and possibly direct deleterious interactions, the relative contribution of each varying according to the NP composition and surface chemistry. Their wide use in public and industrial domains requires a good understanding and even a good control of their toxicity. To address this question, we engineered ZnO QDs with different surface chemistries, expecting that they would exhibit different photo-induced reactivities and possibly different levels of interaction with biological materials. No photo-induced toxicity could be detected on whole bacterial cell toxicity assays, indicating that ROS-dependent damages, albeit real, are hidden behind a stronger source of toxicity, which was comforted by the fact that the different ZnO QDs displayed the same level of cell toxicity. However, using in vitro DNA damage assays based on quantitative PCR, significant photo-induced reactivity could be measured precisely, showing that different NPs exhibiting similar inhibitory effects on whole bacteria could differ

dramatically in terms of ROS-generated damages on biomolecules. We propose that direct interactions between NPs and bacterial cell surfaces prime over any kind of intracellular damages to explain the ZnO QDs toxicity on whole bacterial cells.

1. INTRODUCTION

Late developments in nanotechnologies are experiencing such progresses that they led to the engineering of a plethora of nanoparticles (NPs) with unique properties already fulfilling various tasks in modern life as they massively enter in industrial processes and consumer products [1,2]. Among them, metal oxide NPs, such as zinc oxide (ZnO) NPs, are currently focusing considerable attentions due to their high potential for applications such as catalysis, sensing and environmental remediation [3-6]. Nevertheless, the outstanding properties associated to the nanoscale of these particles has led to the rapid development of innovative technologies that surpasses the full understanding of the adverse effects of nanomaterials when health and environmental impacts are considered. However, gaining a wide public acceptance for such NPs necessarily implies a deep knowledge and a fine control of their toxicity in order to limit the risks for human and environmental health.

Regarding metal oxide toxicity, a plethora of reports are regularly opposing the production of reactive oxygen species (ROS), the release of metal cations and even direct interaction between the NPs and the cell surface, a long standing debate that reflects the complexity of the underlying toxicity mechanisms involved [7-15]. The toxicity of ZnO NPs may be partially attributed to the dissolution of the nanocrystals, which depends on pH, on the size of the particles and on the medium composition, and the associated release of Zn^{2+} ions may enter the cells and damage cellular components such as proteins and DNA [16-18]. Recent reports highlight also the key role played by the ROS generated by ZnO NPs under light irradiation and even in the dark [8,9,19-23]. ZnO is a semiconductor with a bandgap of 3.37 eV in the bulk state and is able to be activated by wavelengths equal of below 368 nm. The associated oxido-reduction reactions occurring with O_2 and H_2O at the surface of ZnO NPs generate hydroxyl ($^{\bullet}OH$), superoxide ($O_2^{\bullet-}$) and hydroperoxyl ($HO_2^{\bullet}$) radicals and H_2O_2 that cause membrane damages by lipid peroxidation [24]. Moreover, these membrane damages favor the internalization of ZnO NPs and lead to cell death. Noteworthy is also that these photo-generated ROS not only oxidize chemical and biological species located in the vicinity of the NPs but may also affect the ligands at the periphery of the NPs and cause NPs aggregation and/or dissolution [25,26]. Although the photoxicity of ZnO NPs is directly

related to the level of ROS produced, it also depends on the proximity between the source of ROS and the cells, and thus the level of interaction between the cells and the NP for which the surface chemistry is a key parameter [27]. Clearly, future developments of metal oxide-based nanotechnologies will require a better understanding of the different sources of toxicity and their relative contribution, in order to engineer NPs of controlled and predictable toxicity.

In this study, we investigated the relationship between the surface chemistry of ZnO core QDs and the toxicity of the nanoparticles against *Escherichia coli* using whole cell assays. Although surprising, different ZnO core QDs exhibiting different levels of reactivity did not differ significantly in terms of toxicity when assessed using whole cell luminescent biosensors. This led us to develop a molecular-based assay where DNA degradation was used as surrogate to evaluate the level of ROS-generated damages on biomolecules. This approach allows pointing out different levels of deleterious effects that were otherwise undetectable when using whole cell toxicity assays.

2. MATERIALS AND METHODS

2.1. Synthesis of ZnO core QDs and evaluation of their stability

3-Aminopropyltrimethoxysilane (APTMS), (3-glycidyloxypropyl)trimethoxysilane (GLYMO) and the sulfobetaine zwitterionic (SBZ) ligand were used to disperse oleate-capped ZnO QDs in water (Fig. 1). The synthetic protocols used to prepare ZnO@APTMS, ZnO@GLYMO, ZnO@SBZ QDs are detailed in the Supporting Information. ZnO QDs were characterized by transmission electron microscopy (TEM), X-ray diffraction (XRD), X-ray photoelectron spectroscopy (XPS) and UV-visible and fluorescence spectroscopy.

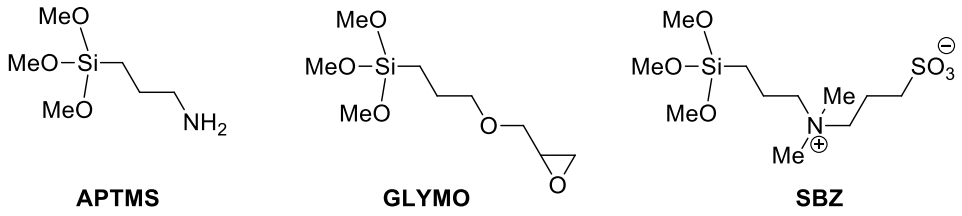

Fig. 1. Structures of the APTMS, GLYMO and SBZ ligands used to disperse ZnO QDs in water.

The stability of the ZnO QDs with respect to dissolution was assessed by measuring the amount of leaked Zn^{2+} (ICP-OES) recovered from the dialysate of an 8–10 kD dialysis device (Float-A-Lyzer G2; Spectra/Por), see Supporting information for details [14].

2.2. Evaluation of QDs-generated ROS

The amount of $^{\bullet}OH$, $O_2^{\bullet-}$ radicals and of H_2O_2 produced by the QDs, with or without photo-induction, were determined using disodium terephthalate (DST), nitroblue tetrazolium (NBT) and crystal violet/horseradish peroxidase assays, respectively, as already reported by Moussa *et al*. [23] (Supporting information). All experiments were conducted using aqueous dispersions of QDs with an UV-visible absorption of 0.1 at 330 nm. Results were corrected relative to the Zn content of each sample determined by inductively coupled plasma-optical emission spectrometer (ICP-OES) analyses. ROS measurements were mostly carried out in water and cannot be transposed directly into a possible toxicity level against bacteria in culture media as production of ROS and their availability are influenced by the surrounding biological medium. Nevertheless, comparative assays made using the ZnO@APTMS QDs showed that photogenerated-ROS detected in MOPS culture medium were about 30% of the value measured in water (Supporting information, section 2.4), which remains far from being negligible.

2.3. Evaluation of ZnO QDs toxicity

Toxicity tests on live bacterial cells were based on bioluminescence extinction assays of the *E. coli* strain MG1655(pUCD07) as described elsewhere [14] (see Supporting information). Typically, the luminescent bacterium was cultivated in a MOPS mineral medium known to limit metal chelation, and supplemented with gluconate as sole carbon source. Cultures were exposed to a set of ZnO QDs, with or without exposure of a full spectrum neon lighting (18W T8 “Solar Reptil Sun” from JBL, illuminance ca. 9 klux). The extinction of the bacterial luminescence was recorded on plate reader and normalized to the biomass (OD600).

2.4. Evaluation of QD-generated stresses

Exposure to free Zn^{2+}, oxidative stress or DNA damaging stress, were assessed using whole cell biosensor assays with dedicated *E. coli* strains. These consist of genetically modified bacteria specifically engineered to emit a bioluminescent signal when the stress is perceived by the live bacteria (transcriptional fusions of regulated promoters to lux reporter genes). Strains construction and use are detailed in the Supporting information.

2.5 Assessing QDs reactivity against DNA

Photo-induced damage to DNA assays consisted in exposing 500 ng of a well-defined pBELX plasmid DNA [28], for 10 min, to known concentrations of ZnO QDs, with or without exposure to a full spectrum neon lighting as described for the toxicity test. The exposed DNA was further purified using a QIAquick® PCR purification kit (Qiagen) and used as template for the quantification of unaltered molecules by qPCR (Supporting information). DNA treated similarly with free Zn^{2+} did not show significant damage nor recovery limitation.

3. RESULTS AND DISCUSSION

3.1. ZnO QDs synthesis and characterization

Oleic acid-capped ZnO QDs were prepared via a sol-gel process according to our previous reports [ref]. To disperse the hydrophobic NPs in aqueous solution, a ligand exchange was conducted using 3-aminopropyltrimethoxysilane (APTMS), (3-glycidyloxypropyl)trimethoxysilane (GLYMO) or with a sulfobetaine zwitterionic (SBZ) ligand (Fig. 1) in order to engineer NPs presenting different level of photo-induced ROS production, as well as different surface chemistries enabling to develop different types of interactions with bacterial cells (Supporting Information).

The size and the shape of ZnO QDs were characterized by TEM (Fig. 2a-c). The micrographs show that the dots were relatively monodispersed and the average size of the spherical/ellipsoidal NPs is of ca. 4-5 nm. The clear lattice fringes and the selected area electron diffraction patterns (SAED) (insets of Fig. 2a-c) indicate the good crystallinity of

ZnO QDs. This was further confirmed by the XRD patterns of ZnO QDs in which the diffraction peaks could well be indexed to the wurtzite structure of ZnO (space group $P6_3mc$, JCPDS No 36-1451) (Fig. 3). The broad peaks observed for all samples further confirm the small size of ZnO NPs.

The UV-visible absorption spectra of ZnO QDs are shown in Fig. 2d-f and the excitonic peaks are nearly located at the same wavelength (ca. 336 nm), further confirming that ZnO QDs functionalized by APTMS, GLYMO or SBZ exhibit the same size. The excitonic absorption of bulk ZnO appears at ca. 380 nm (3.26 eV), value significantly higher than those determined for ZnO QDs, indicating the spatial confinement of the charge carriers in these nanocrystals. Using the experimental formula [ref]:

$$1240/\lambda_{1/2} = a + b/D^2 - c/D$$

where $\lambda_{1/2}$ is the wavelength corresponding to an absorption of 50% to that of the excitonic peak and a,b and c are parameters for ZnO QDs with diameters in the 2.5-6.5 nm range, the diameters D of ZnO@APTMS, GLYMO and SBZ QDs were estimated to be xx, yy, and zz nm, respectively, values in good agreement with those determined by TEM. Finally, due to the intrinsic defects present in ZnO QDs prepared by a sol-gel method, the photoluminescence (PL) spectra only exhibit deep-level visible emission centered at 557, 565 and 559 nm for of ZnO@APTMS, GLYMO and SBZ QDs, respectively (Fig. 2d-f). These emissions originate from an electronic transition from a level close to the conduction band edge to a defect associated trap state (oxygen vacancies, interstitial zinc sites or donor-acceptor pairs).The PL quantum yields of ZnO@APTMS, GLYMO and SBZ QDs in water were determined to be 21, 25 and 17%.

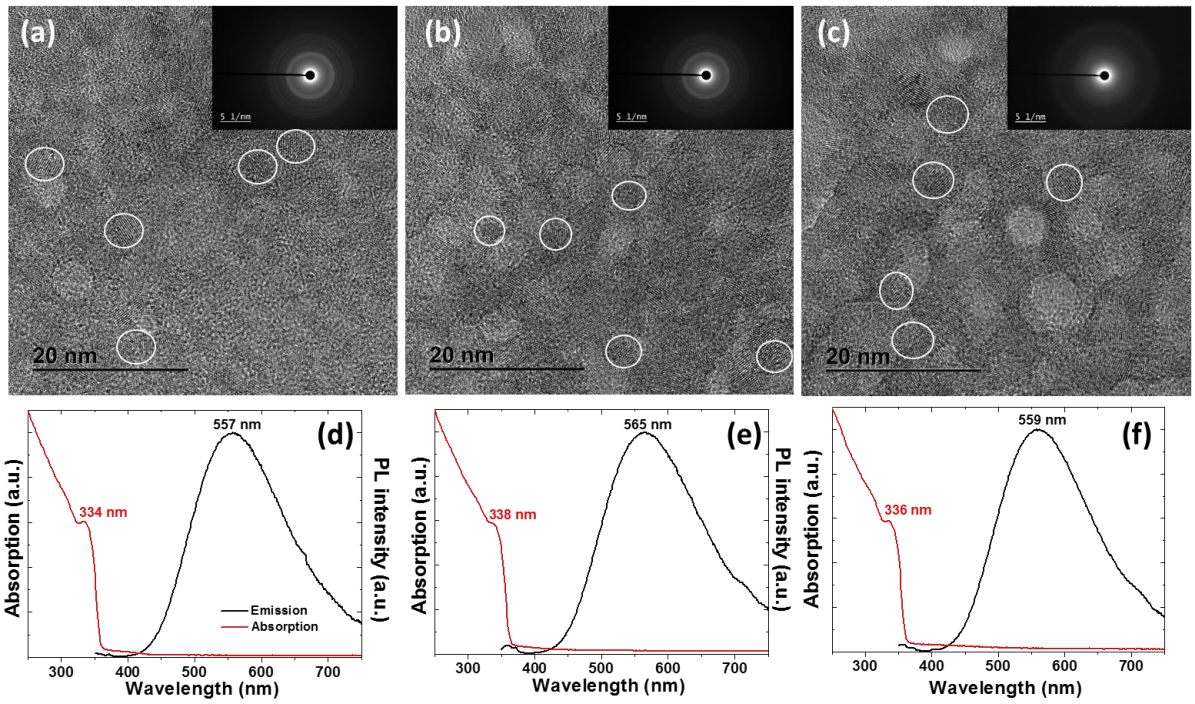

Fig. 2. TEM images of (a) ZnO@APTMS, (b) ZnO@GLYMO and (c) ZnO@SBZ QDs (the insets are the SAED patterns). UV-visible absorption and PL emission spectra of (d) ZnO@APTMS, (e) ZnO@GLYMO and (f) ZnO@SBZ QDs (the excitation wavelength is 330 nm).

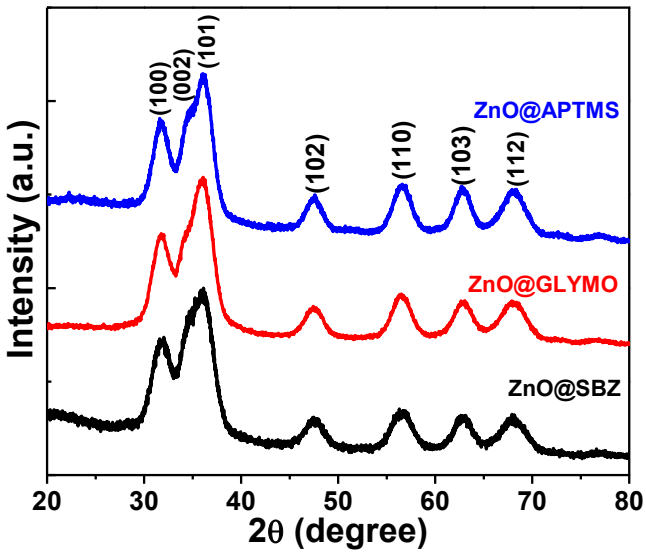

Fig. 3. XRD patterns of ZnO QDs functionalized with APTMS, GLYMO or SBZ.

3.2. Surface chemistry-dependent ROS production of ZnO QDs

In this study, the toxicity of NPs-generated ROS was explored on the bacterial system, using a set of ZnO core QDs. Four nanometer-sized ZnO core QDs were functionalized with either 3-aminopropyltrimethoxysilane (APTMS), (3-glycidyloxypropyl)trimethoxysilane (GLYMO) or with a sulfobetaine zwitterionic (SBZ) ligand (Fig. 1) in order to engineer NPs presenting different level of photo-induced ROS production, as well as different surface chemistries enabling to develop different types of interactions with bacterial cells (Supporting information, section 1). The three QDs exhibited different levels of photo-induced ROS production (Fig. 1), therefore highlighting the importance of their surface chemistry on their photoreactivity and possibly their toxicity if ROS production is to be concerned.

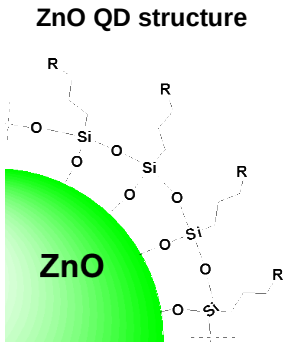

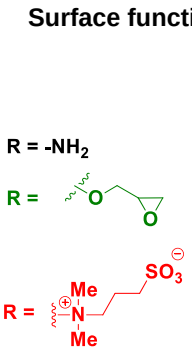

ROS production (µM)

	$[H_2O_2]$	$[O_2^{\bullet-}]$	$[^{\bullet}OH]$
ZnO@APTMS	19	161	980
ZnO@GLYMO	71	148	1490
ZnO@SBZ	70	330	220

Fig. 4. Structure and photo-reactivity of the ZnO core QDs. ZnO@APTMS, ZnO@GLYMO, and ZnO@SBZ QDs are all silane-based nanoparticles differing only by their surface functionalization (amino groups, epoxides and a zwitterion surface coating respectively). The ROS production following 1 h photoactivation was measured in water using common procedures, and normalized to a same initial QD concentration for comparing ROS production by the three nanoparticles (Supporting information, section 3).

3.2. Toxicity assessment of ZnO QDs on whole bacterial cells

The toxicity of the three ZnO QDs was evaluated on the *E. coli* strain MG1655(pUCD607) using a bioluminescence extinction assay. A first set of experiments, carried out in the dark, showed that the QDs exhibit similar toxicities, with Minimum Inhibitory Concentration (MIC) values ranging from 1.8×10^{-4} to 2.9×10^{-4} MZnEq (molar concentration of zinc equivalent). Noteworthy is that ZnO QDs are ca. twice less toxic than their equivalent content in Zn^{2+} as seen with a $ZnCl_2$ control (MIC $\approx 1\times10^{-4}$ M; Fig. 5). With this respect, a dialysis experiment carried out using ZnO@APTMS QDs at concentration slightly lower than MIC

(ca. 8×10^{-5} MZnEq) demonstrates that the concentration of free Zn^{2+} released does not exceed the "No Observable Effect Concentration" (NOEC) obtained for $ZnCl_2$ (ca. 1×10^{-5} M). This therefore rules out the possibility that the toxic effects observed were solely due to the release of Zn^{2+} originating from the dissolution of QDs or Zn-containing adsorbed complexes (Supporting information). In a second set of experiments, the QDs toxicity against *E. coli* was investigated under simulated sunlight exposure. Despite a marked difference regarding their photo-reactivity in terms of ROS production (Fig. 1), no significant difference in toxicity on *E. coli* was observed between the three QDs, where MIC values were similar to those observed in the dark (Fig. 2, Supporting information Fig. S2). Despite stable MIC values, the bioluminescence profiles appeared to evolve with the illumination time. If part of it could be attributed to the photo-sensitivity of bioluminescence production, as demonstrated in Fig. 2D, the NOECs are clearly displaced towards lower concentrations in a QD-dependent manner. It should be observed that according to Fig. 2C, the ZnO@GLYMO QDs, displaying the lowest NOEC value after two hours of illumination, are also the higher hydroxyl radical producers.

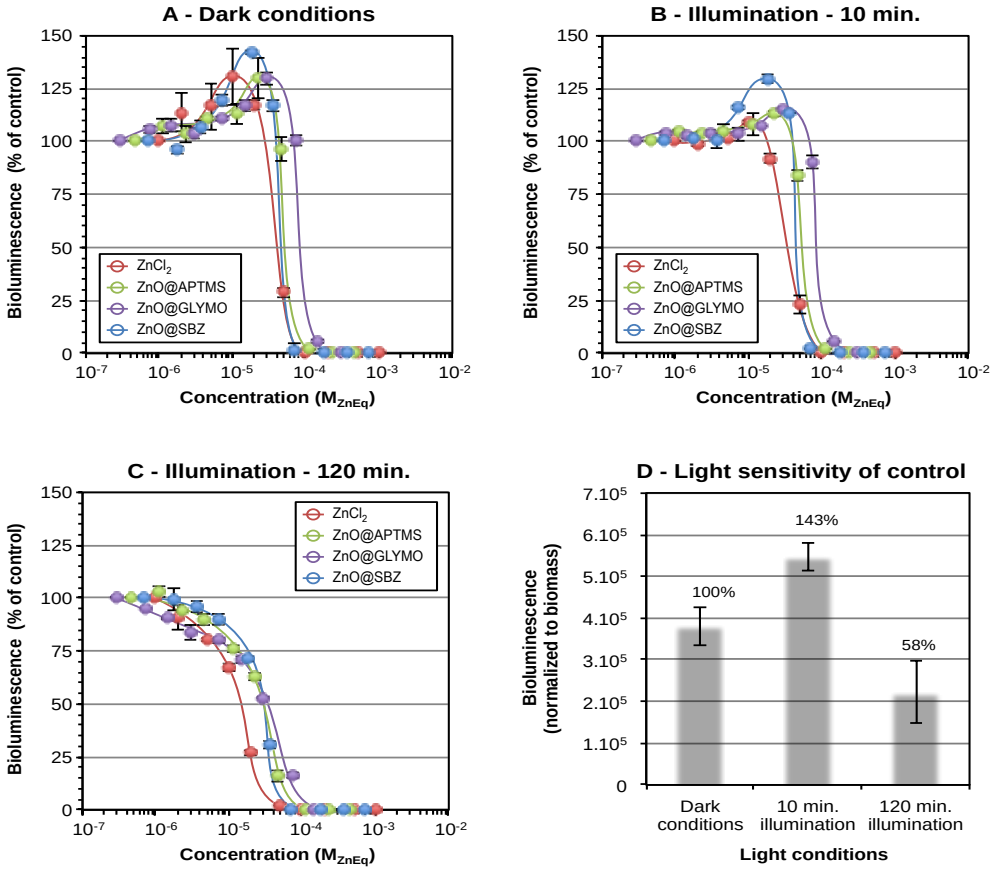

Fig. 2. Effect of light irradiation on ZnO core QD toxicity. Bioluminescence extinction curves of strain *E. coli* MG1655(pUCD607) exposed to $ZnCl_2$, ZnO@APTMS,

ZnO@GLYMO, and ZnO@SBZ QDs maintained in the dark for 2 hours (A), maintained in the dark for 110 min and then exposed to a 10 min illumination (B), or illuminated for 2 h (C). Control assays without $ZnCl_2$ or ZnO QDs amendment displayed a light sensitivity depending of the exposure time (D). Further comparisons are available in the Supporting information. Error bars represent minimum and maximum values of two independent sets of experiments for (A), (B), (C), and standard deviation (n=8) for (D).

3.3. Stress assessment using whole cell biosensor assays

When considering the results of the bioluminescence-based toxicity tests, it clearly appears that (i) the three ZnO QDs are less toxic than their Zn content, and (ii) the levels of Zn^{2+} leaking from the NPs are so low (Supporting information Fig. S1) that QDs dissolution cannot be considered as a significant source of toxicity by itself. If Zn^{2+} leakage is of limited incidence, it is tempting to propose ROS production as an alternative source of toxicity. However, the stable MIC values observed regardless of the illumination conditions would rather be in favor of a non-ROS-based toxicity. An elucidation of this dilemma was attempted using a set of specific *E. coli* whole cell biosensors for Zn^{2+}, oxidative stress, and DNA damages (Supporting information, section 6), in order to identify which cell stress dominates when bacterial cells are exposed to ZnO QDs. The use of such biosensors non-ambiguously demonstrated that only Zn^{2+} ion leakage was perceived by the bacteria (Supporting information Fig. S3C and S3D), although Zn^{2+} concentration was too low to explain the QD toxicity by itself. In addition, even if the three ZnO QDs produce ROS, no oxidative stress response was observed using a dedicated biosensor (Supporting information Fig. S3A). All together, the relative stability of the NPs and the absence of photo-induced toxicity tend to show that neither Zn^{2+} leakage nor ROS production are responsible for the QDs toxicity. This necessarily implies an alternative source of toxicity, which is not without reminding previous suggestions regarding the deleterious effect of direct cell-NPs interactions [10,12,13]. Still, the absence of ROS-induced stress response in the whole cell biosensors may be surprising as ROS production could be measured for all QDs (Fig. 1). Since ROS are produced extracellularly, cell impairments caused by the oxidative damages of bacterial surface structures are likely to occur before cells could trigger any detectable stress response. Alternatively, the non-ROS non-Zn^{2+} toxicity mentioned before may dominate the QDs toxicity, which leads to strong cell damages that preclude subsequent oxidative stress response to be triggered. At this stage, the level of damages generated by photo-induced ROS remains an open question.

3.4. Setting up a DNA degradation assay to assess QD photo-induced reactivity

Apart from being limited to settings allowing physiological conditions, the use of live material for toxicity testing requires that cells should be able to respond before being too damaged. On the principle, this could be overcome if the analytical procedures focus on the alteration of biological material by itself rather than the alteration of the cell functioning. In the next series of experiments, DNA was used as a surrogate biomolecule to estimate the QDs injuriousness at elevated concentrations (to prevent high dissolution rate), and in non-physiological medium (to limit ROS scavenging if any). Five hundred ng fractions of H_2O-dissolved DNA (plasmid pBELX) were independently exposed for 10 min to each of the QDs at concentrations ranging from 1.5 to 1.8 ×10-3 MZnEq, in the dark or under light irradiation. An agarose gel electrophoresis of the mixtures clearly showed that in the dark, the QDs had no effect on DNA integrity (Fig. 3A). Only in the case of the ZnO@APTMS QDs, both a plasmid band reduction and a fluorescent smear above the plasmid band indicate a strong interaction between the DNA and the QDs leading to a gel retardation. Conversely, a 10 min light irradiation had a dramatic effect on DNA integrity where fluorescent smears below the normal plasmid band size indicate random DNA fragmentation and thus severe DNA damages. The levels of DNA alteration were further measured by quantitative PCR (qPCR), considering that a full DNA integrity is a prerequisite for a proper PCR-amplification to proceed. Analyses of DNA integrity by qPCR, after purification of the QDs-exposed DNA, showed that, in the dark, ZnO@APTMS and ZnO@SBZ QDs poorly altered pBELX DNA (ca. 75% integrity) while only 4% of undamaged DNA could be recovered after exposure to ZnO@GLYMO. A 10 min light irradiation resulted in dramatic effects on DNA integrity, with ca. 0.4-0.5% of unaltered pBELX recovered after exposure to ZnO@APTMS and ZnO@SBZ QDs, and as low as 0.02% recovery in the case of the ZnO@GLYMO QDs. These experiments clearly indicate that (i) despite being undetected in whole cell-based toxicity tests, ZnO QDs could cause severe photo-induced damages on biomolecules, and (ii) the levels of photo-induced damages observed partially follow the levels of ROS generated by the various NPs, with ZnO@GLYMO being both the more reactive and the more damaging QDs.

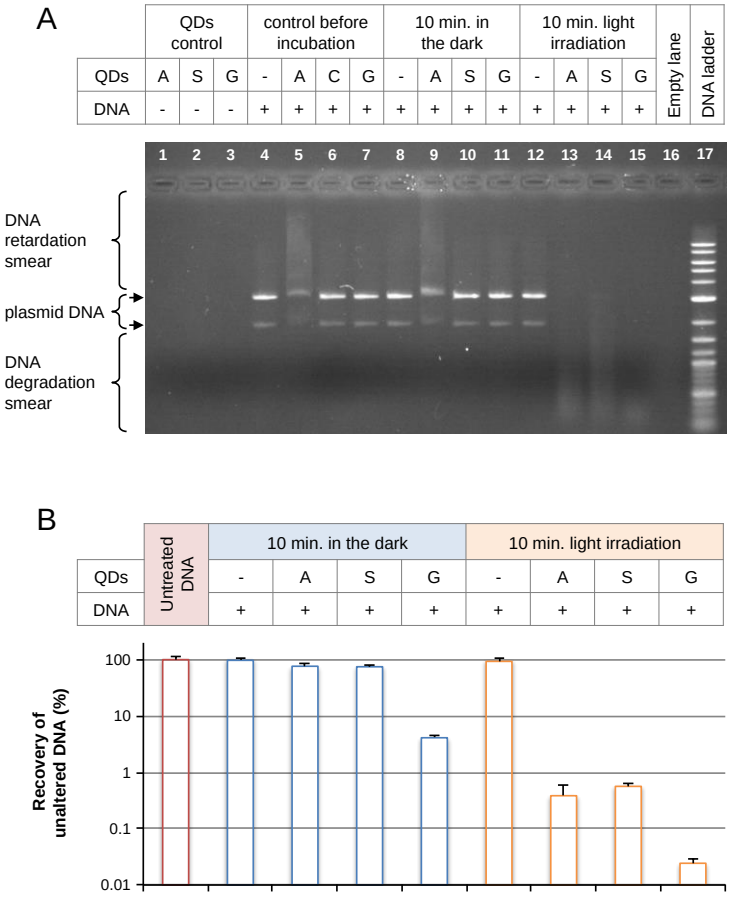

Fig. 3. Photo-induced DNA damages by ZnO QDs. a, Alteration of pBELX plasmid DNA22 (3169 bp) upon exposure to ZnO@APTMS (A), ZnO@SBZ (S), and ZnO@GLYMO (G) for 10 min with or without light irradiation (full spectrum white light, 9 klux illuminence) and the mixture was run on a 1% agarose gel in TAE buffer. DNA was stained with ethidium bromide and "2log DNA ladder" (New England Biolabs®) was used as DNA molecular weight marker. An image analysis (Image Lab™ Software, Gel Doc™, Bio-Rad) shows that the total amount of the fluorescence is conserved between lane except for from lanes #13, #14, #15, where only 40% to 10% of the fluorescence is kept, indicating a pure loss of DNA material. b, Quantification of pBELX DNA integrity following a 10 min exposure to ZnO@APTMS (A), ZnO@SBZ (S), and ZnO@GLYMO (G) at 1.6×10-3, 1.5×10-3, and 1.8×10-3 MZnEq respectively, with or without light irradiation. DNA integrity was estimated by qPCR and is given as a fraction (% recovery) of what obtained for untreated DNA controls. Error bars represent standard deviations of 6 values (2 independent experiments with triplicate qPCR assays each).

4. CONCLUSIONS

In conclusion, using a set of differently functionalized ZnO QDs, NPs generating various levels of photo-induced ROS could be engineered. Although the highest ROS producers QDs

(ZnO@GLYMO) were the most damaging towards DNA, the levels of photo-induced damages did not fully correlate with the ROS production, indicating that alternative phenomena such as QD-biomolecule interactions might also contribute to the overall NP reactivity. However, if all ZnO QDs were undoubtedly very photo-reactive towards a surrogate biomolecule (DNA), no clear photo-induced toxicity could be observed in whole bacterial cells toxicity assays. This likely illustrates the barrier effect exerted by numerous biomolecules present on cell surfaces that prevent the ROS produced to reach critical cell functions. With this respect, it is worth mentioning that, contrary to eukaryotic cells, bacteria do not practice endocytosis and QDs have to cross several external barriers before reaching vital functions, suggesting that only closely delivered ROS could be effective. While the ROS did not appear to be directly involved in the cell toxicity observed for the studied ZnO QDs, it was quite surprising to observe that the free Zn^{2+} leaked by the QDs did not reach the critical level where cell functioning could be impaired. Considering that both ROS production and Zn^{2+} leaks are insufficient to impair cell functioning, a third source of toxicity has to be considered. Taking into account the nanoscale dimensions of the particles, direct and deleterious interactions of the NPs with important extracellular/periplasmic cell components (e.g. respiratory chain, transporters) could well be a plausible explanation to explore. Whatever the toxicity mechanisms involved, this study emphasizes the fact that toxicity tests carried out on live bacterial cells are likely inappropriate for evaluating NP generated-ROS deleterious effects. For that reason, the DNA-damaging test we propose here advantageously offers (i) the possibility of quantifying photo-induced damages on a biomolecule without making use of live cells therefore avoiding interfering parameters such as NP internalization or bio-generated ROS, (ii) to work in non-physiological conditions, e.g. in water, thus avoiding ROS scavenging for instance, and (iii) to work at NP concentrations well over the toxic level if necessary.

ACKNOWLEDGMENT

This work was supported by the program CESA of the French National Research Agency (ANR) (Project “NanoZnOTox”; ANR-11-CESA-0004ANR). Additional support was gained from the Hydreos competitiveness cluster. The authors wish to thank Hervé Marmier (LIEC, Université de Lorraine) for ICP-OES analyses, Ghouti Medjhadi (IJL, University de Lorraine) for XRD analyses and Mathieu Lhuire for technical assistance.

APPENDIX A. SUPPLEMENTARY DATA

Supplementary data associated with this article can be found, in the online version.

REFERENCES

1. C.A. Charitidis, P. Georgiou, M.A. Koklioti, A.-F. Trompeta, V. Markakis. Manufacturing nanomaterials: from research to industry. Manufacturing Rev. 1 (2014) 11.

2. W.J. Stark, P.R. Stoessel, W. Wohlleben, A. Hafnerc. Industrial applications of nanoparticles. Chem. Soc. Rev. 44 (2015) 5793-5805.

3. Z.L. Wang. Zinc oxide nanostructures: growth, properties and applications. J. Phys.: Condens. Matter 16 (2004) R829-R858.

4. H. Moussa, E. Girot, K. Mozet, H. Alem, G. Medjahdi, R. Schneider. ZnO rods/reduced graphene oxide composites prepared via a solvothermal reaction for efficient sunlight-driven photocatalysis. Appl. Catal. B: Environ. 185 (2016) 11-21.

5. X. Liu, J. Zhang, L. Wang, T. Yang, X. Guo, S. Wu, S. Wang. 3D hierarchically porous ZnO structures and their functionalization by Au nanoparticles for gas sensors. J. Mater. Chem. 21 (2011) 349-356.

6. M.M. Khin, A. Sreekumaran Nair, V. Jagadeesh Babu, R. Murugana, S. Ramakrishna. A review on nanomaterials for environmental remediation. Energy Environ. Sci. 5 (2012) 8075-8109.

7. Y. Li, W. Zhang, J. Niu, Y. Chen. Mechanism of photogenerated reactive oxygen species and correlation with the antibacterial properties of engineered metal-oxide nanoparticles. ACS Nano 6 (2012) 5164-5173.

8. H. Ma, L.K. Wallis, S. Diamond, S. Li, J. Canas-Carrell, A. Parra. Impact of solar UV radiation on toxicity of ZnO nanoparticles through photocatalytic reactive oxygen species (ROS) generation and photo-induced dissolution. Environ. Pollut. 2014, 193, 165-172.

9. V.L. Prasanna, R. Vijayaraghavan. Insight into the mechanism of antibacterial activity of ZnO: Surface defects mediated reactive oxygen species even in the dark. Langmuir 31 (2015) 9155-9162.

10. A.B. Djurišić, Y.H. Leung, A.M. Ng, X.Y. Xu, P.K. Lee, N. Degger, R.S. Wu. Toxicity of metal oxide nanoparticles: mechanisms, characterization, and avoiding experimental artefacts. Small 11 (2015) 26-44.

11. J. Ying, T. Zhang, M. Tang Metal Oxide Nanomaterial QNAR Models: available structural descriptors and understanding of toxicity mechanisms. Nanomaterials (Basel) 5 (2015) 1620–1637.

12. Y.H. Leung, A.M. Ng, X. Xu, Z. Shen, L.A. Gethings, M.T. Wong, C.M. Chan, M.Y. Guo, Y.H. Ng, A.B. Djurišić, P.K. Lee, W.K. Chan, L.H. Yu, D.L. Phillips, A.P. Ma, F.C. Leung. Mechanisms of antibacterial activity of MgO: non-ROS mediated toxicity of MgO nanoparticles towards Escherichia coli. Small 10 (2014) 1171-1183.

13. K. Feris, C. Otto, J. Tinker, D. Wingett, A. Punnoose, A. Thurber, Kongara, M., M. Sabetian, B. Quinn, C. Hanna, D. Pink. Electrostatic interactions affect nanoparticle-mediated toxicity to gram-negative bacterium *Pseudomonas aeruginosa* PAO1. Langmuir, 26 (2010) 4429-4436.

14. X. Bellanger, P. Billard, R. Schneider, L. Balan, C. Merlin. Stability and toxicity of ZnO quantum dots: interplay between nanoparticles and bacteria. J. Hazard. Mater. 283 (2015) 110-116.

15. J. Ying, T. Zhang, M. Tang. Metal Oxide Nanomaterial QNAR Models: available structural descriptors and understanding of toxicity mechanisms. Nanomaterials (Basel) 5, (2015) 1620–1637.

16. J.A. Lemire, J.J. Harrison, R.J. Turner. Antimicrobial activity of metals: mechanisms, molecular targets and applications. Nat. Rev. Microbiol. 11 (2013) 371-384.

17. W. Song, J. Zhang, J. Guo, J. Zhang, F. Ding, L. Li, , Z. Sun. Role of the dissolved zinc ion and reactive oxygen species in cytotoxicity of ZnO nanoparticles. Toxicol. Lett., 199 (2010) 389-397.

18. M. Li, L. Zhu, D. Lin. Toxicity of ZnO Nanoparticles to *Escherichia coli*: mechanism and the influence of medium components. Environ. Sci. Technol. 45 (2011) 1977–1983.

19. G. Applerot, A. Lipovsky, R. Dror, N. Perkas, Y. Nitzan, R. Lubart, A. Gedanken, Enhanced antibacterial activity of nanocrystalline ZnO due to increased ROS-mediated cell injury. Adv. Funct. Mater. 19 (2009) 842–852.

20. D. Wang, L. Zhao, H.Ma, H. Zhang, L.-H. Guo. Quantitative analysis of reactive oxygen species photogenerated on metal oxide nanoparticles and their bacteria toxicity: the role of superoxide radicals. Environ. Sci. Technol. 51 (2017) 10137−10145.

21. X. Jiang, W. He, X. Zhang, Y. Wu, Q. Zhang, G. Cao, H. Zhang, J. Zheng, T.R. Croley, J.-J. Yin. Light-induced assembly of metal nanoparticles on ZnO enhances the generation of charge carriers, reactive oxygen species, and antibacterial activity. J. Phys. Chem. C 122 (2018) 29414−29425.

22. C. Mao, Y. Xiang, X. Liu, Z.Cui, X. Yang, K.W.K. Yeung, H. Pan, X. Wang, P.K. Chu, S. Wu. Photo-inspired antibacterial activity and wound healing acceleration by hydrogel embedded with Ag/Ag@AgCl/ZnO nanostructures. ACS Nano 11 (2017) 9010−9021.

23. H. Moussa, C. Merlin, C. Dezanet, L. Balan, G. Medjahdi, M. Ben-Attia, R. Schneider. Trace amounts of Cu^{2+} ions influence ROS production and cytotoxicity of ZnO quantum dots. J. Hazard. Mater. 304 (2016) 532-542.

24. R.K. Dutta, B.P.Nenavathu, M.K. Gangishetty, A.V.R. Reddy. Studies on antibacterial activity of ZnO nanoparticles by ROS induced lipid peroxidation. Colloids Surf. B: Biointerfaces 94 (2012) 143-150.

25. J. Ma, J.-Y. Chen, Y. Zhang, P.-N. Wang, J. Guo, W.-L. Yang, C.-C. Wang. Photochemical instability of thiol-capped CdTe quantum dots in aqueous solution and living cells: process and mechanism. J. Phys. Chem. B 111 (2007) 12012–12016.

26. F.A. Kauffer, C.Merlin, L. Balan, R. Schneider. Incidence of the core composition on the stability, the ROS production and the toxicity of CdSe quantum dots, J. Hazard. Mater. 268 (2014) 246-255.

27. M. Arakha, M. Saleem, B.C. Mallick, S. Jha. The effects of interfacial potential on antimicrobial propensity of ZnO nanoparticle. Sci. Rep. 5 (2015) 9578.

28. X. Bellanger, H. Guilloteau, B. Breuil, C. Merlin. Natural microbial communities supporting the transfer of the IncP-1β plasmid pB10 exhibit a higher initial content of plasmids from the same incompatibility group. Front. Microbiol. 5 (2014) 637.